

Measurement of Z/γ^* +jet+X and $\gamma+b/c+c$ +X Cross Sections with the D0 Detector

Murilo RANGEL^{*}

Laboratoire de l'Accélérateur Linéaire

E-mail: rangel@fnal.gov

on behalf of D0 collaboration

We present measurements of differential cross sections for the inclusive Z/γ^* + jet production and the inclusive photon plus heavy flavor production in a data sample of 1fb^{-1} collected with the DØ detector in proton-antiproton collisions at $\sqrt{s}=1.96$ TeV. In the first measurement, we compare kinematic distributions of the Z/γ^* and the jets as well as various angles of the Z +jet system with different Monte Carlo event generators and next-to-leading order perturbative QCD (NLO pQCD) predictions with non-perturbative corrections applied. In the second measurement, we compare the results with NLO pQCD predictions, covering photon transverse momenta 30-150 GeV, photon rapidities $|y^\gamma| < 1.0$, jet rapidities $|y^{jet}| < 0.8$, and jet transverse momenta $p_T^{jet} > 15$ GeV.

*European Physical Society Europhysics Conference on High Energy Physics
July 16-22, 2009
Krakow, Poland*

^{*}Speaker.

1. Introduction

Understanding the background productions in searches for new physics is very challenging at hadron colliders. Therefore, measurements of differential cross sections represent important milestones in the discovery road. In this note, we present measurements of $Z/\gamma^* + \text{jets}$ production and photon plus heavy flavor jets at the Fermilab Tevatron with the DØ detector [1].

The production of vector bosons is an important signal at hadron colliders, providing unique information about the production mechanism of heavy bosons with additional hard partons. The electron and muon decay modes are distinct experimental signatures, and can be identified with low background rates.

Photons produced in association with heavy quarks (c or b) at hadron colliders provide valuable information about the heavy quark and gluon content of the initial state hadrons, . Although the background rates are not negligible, the statistics are high enough to constrain accurately the parton distribution functions (PDFs).

2. $Z/\gamma^* + \text{jets}$

The DØ collaboration has studied the production of $Z/\gamma^* + \text{jets}$ in both the electron channel and the muon channel [2, 3, 4]. The jets were reconstructed using a seeded mid-point cone algorithm [5] with cone size of 0.5, and they are required to have $|y| < 2.8$ and $p_T > 20 \text{ GeV}$.

The muons were selected to have opposite charge, $p_T > 15 \text{ GeV}$, $|\eta| < 1.7$ and the di-muon invariant mass ranging between 65 GeV and 115 GeV. Isolation requirements were used to reduce the background rates to negligible levels. The electrons were selected to have opposite charge, $p_T > 25 \text{ GeV}$, $|\eta| < 1.1$ or $1.5 < |\eta| < 2.5$, and the di-electron invariant mass ranging between 65 GeV and 115 GeV. In the muon decay channel, we measured differential cross section in the leading (transverse momenta) jet p_T and the $Z/\gamma^* p_T$ [2]. In Figure 1, the NLO pQCD predictions and from three event generators (ALPGEN [6], using PYTHIA [7] for the showering; SHERPA [8]; PYTHIA, with all jets coming from the parton shower) are compared to data.

The $\Delta\phi$ between the Z/γ^* and the leading jet were also measured in the muon channel using two different p_T thresholds (25 GeV and 45 GeV), since the production of additional jets is essentially uncorrelated with the Z/γ^* production [4]. We compared the measurement with NLO pQCD and LO pQCD predictions, and the event generators: SHERPA; HERWIG using JIMMY [9] for multiple parton interactions; PYTHIA with tune QW and with the Perugia tune using the p_T ordered shower; ALPGEN, using the mentioned PYTHIA tunes and HERWIG for the showering (Figure 2).

In the electron decay channel, we measured the jet p_T spectra normalized to the $Z/\gamma^*(\rightarrow e^+e^-) + X$ cross section in different jet multiplicities [3]. The measurements were compared to different theory predictions: NLO pQCD; LO pQCD; PYTHIA using tune QW; PYTHIA using Tune S0; HERWIG using JIMMY; ALPGEN using PYTHIA tune QW; and SHERPA (Figure 3).

The pQCD NLO prediction describes the DØ measurements within uncertainties while the event generators show varying agreement. With more data, these results can be extended and tighter constraints can be placed.

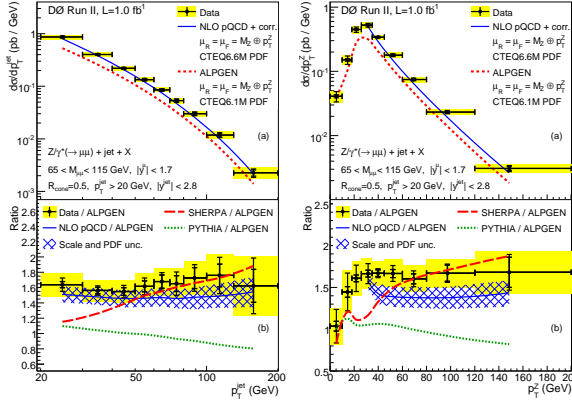


Figure 1: The measured cross section (a) and the ratio of data and predictions to ALPGEN (b) are shown in bins of leading jet p_T (left) and in bins of $Z/\gamma^* p_T$ (right).

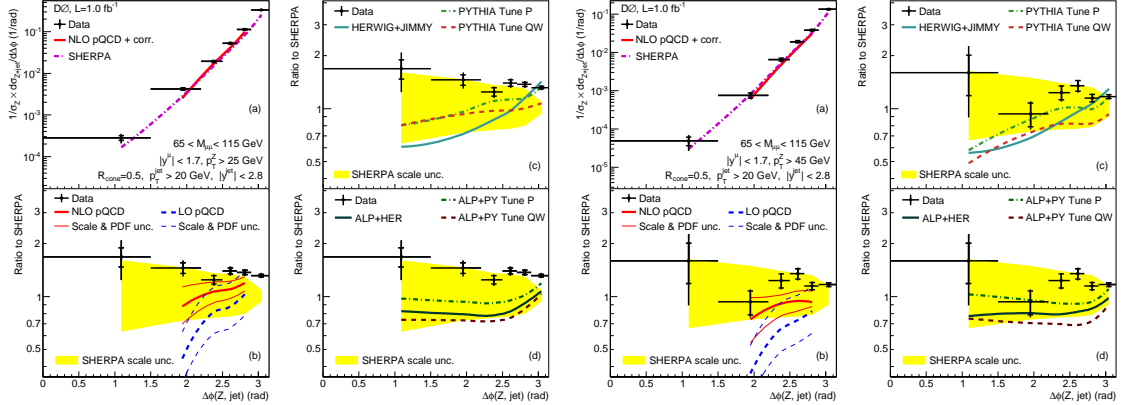


Figure 2: The measured normalized cross section in bins of $\Delta\phi(Z, \text{jet})$ for $Z p_T > 25$ GeV (left) and for $p_T^Z > 45$ GeV (right).

3. Photon+heavy flavor

Using the DØ detector, we studied events with at least one photon candidate and at least one heavy-flavor jet candidate [10]. The photons were selected to have $p_T > 30$ GeV with $|y| < 1.0$ and the leading jet $p_T > 15$ GeV and $|y| < 0.8$. To suppress background events coming from cosmic-ray muons and W leptonic decays, the total missing transverse energy was required to be less than 70% of the photon p_T . The remaining background from dijet events, containing π^0 and η mesons that can mimic photon signatures, is rejected using an artificial neural network (ANN) with the requirement that the ANN output be > 0.7 . Light jets are suppressed using another dedicated ANN (b-ANN), trained to discriminate light flavor from heavy flavor jets. The leading jet is required to have a b-ANN output value > 0.85 .

The fraction of c and b jets in the final data sample is determined using a fitting technique, where the discriminant is $P_b = -\ln \prod_i P_i$, where P_i is the probability of a track in the jet cone to originate from the primary vertex, omitting the least likely track to have come from this vertex.

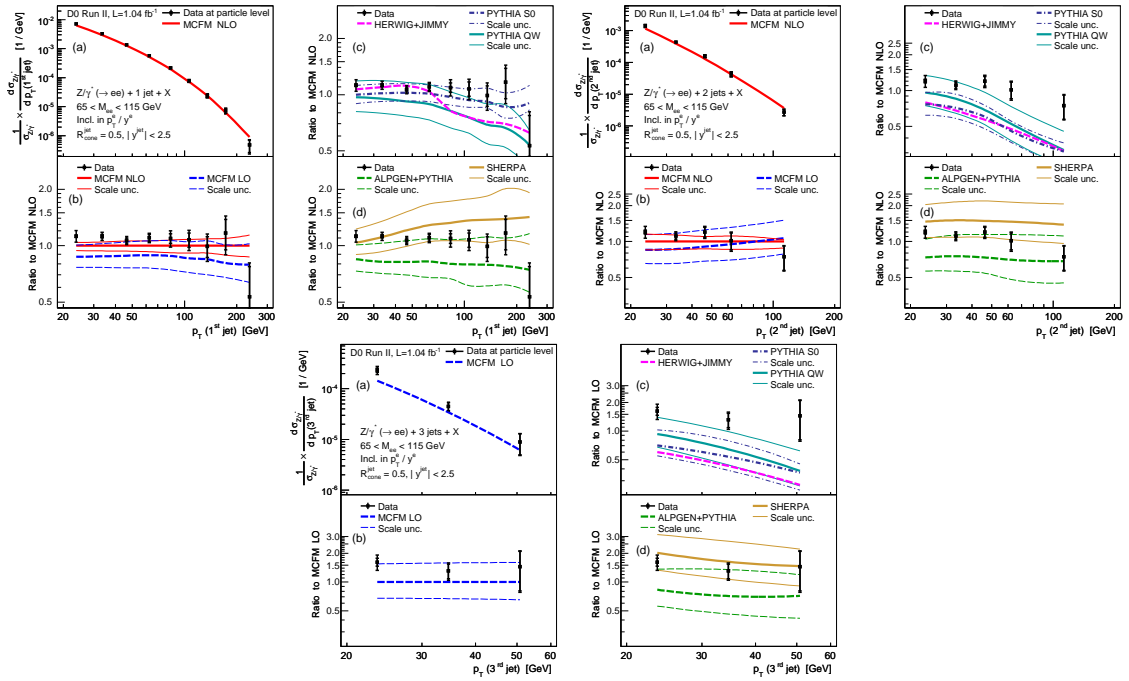


Figure 3: The measured normalized cross section for the leading jet in $Z/\gamma^* + jet + X$ events (upper left) compared to the predictions of NLO and the ratios of data and theory predictions to NLO compared to various event generator models. The measured normalized cross section for the second leading jet in $Z/\gamma^* + 2 jets + X$ events (upper right) compared to the predictions of NLO and the ratios of data and theory predictions to NLO compared to various event generator models. The measured normalized cross section for the third leading jet in $Z/\gamma^* + 3 jets + X$ events (bottom) compared to the predictions of LO and the ratios of data and theory predictions to LO compared to various event generator models.

The measured differential cross sections and their ratios to theoretical predictions are presented in five bins of p_T^γ and two regions of $y^\gamma y^{jet}$ ($y^\gamma y^{jet} > 0$ and $y^\gamma y^{jet} < 0$), and can be seen in Figure 4 for photon + b jets and photon + c jets. Theoretical predictions are from NLO pQCD calculations using the CTEQ 6.6M PDFs. For photon + c jets, comparisons with CTEQ 6.6M PDFs based on the models with an intrinsic charm component (IC) were also done.

The NLO pQCD prediction agrees with the measured cross sections for photon+b production over the entire p_T^γ range, and with photon+c production for $p_T^\gamma < 70$ GeV. For $p_T^\gamma > 70$ GeV, the measured photon + c cross section is higher than the NLO pQCD prediction by about 1.6 - 2.2 standard deviations (including only the experimental uncertainties) with the difference increasing with growing p_T^γ .

4. Conclusion

Important measurements have been performed with the D0 detector, testing NLO pQCD, and the modeling of these complex final states by event generators. The understanding of the discrepancies observed between data and predictions is vital to the sensitivity to new physics at the Tevatron and LHC.

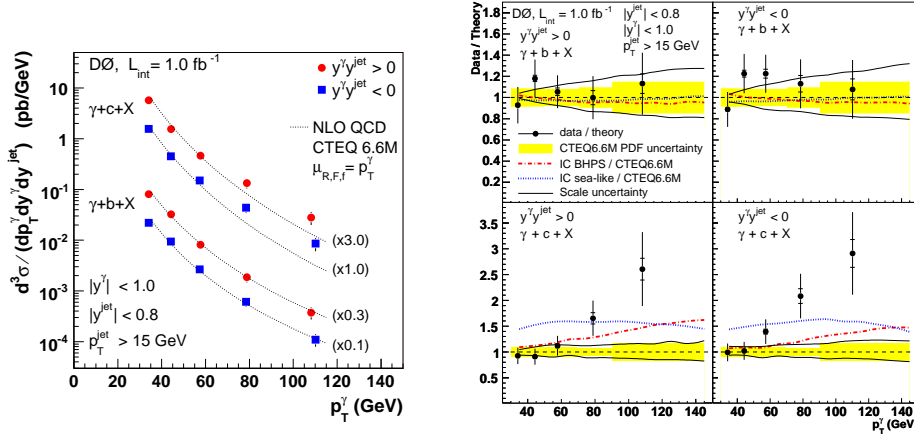


Figure 4: The $\gamma + b$ and $\gamma + c$ differential cross sections as a function of p_T^γ for both rapidity regions. The data points include the overall uncertainties from the measurement, and the theoretical predictions are displayed as dotted lines. The uncertainties from the theoretical predictions include those from the CTEQ 6.6M PDFs (yellow band) and from the choice of scale (full line). The ratio of two intrinsic charm models to the standard theoretical predictions are also included (dashed lines).

References

- [1] V.M. Abazov *et al.* [D0 Collaboration], Nucl. Instrum. Methods Phys. Res. A **565** (2006) 463.
- [2] V. M. Abazov *et al.* [D0 Collaboration], Phys. Lett. B **669** (2008) 278.
- [3] V. M. Abazov *et al.* [D0 Collaboration], Phys. Lett. B **678** (2008) 45.
- [4] V. M. Abazov *et al.* [D0 Collaboration], arXiv:0907.4286 [hep-ex].
- [5] G. C. Blazey *et al.*, Fermilab-Pub-00/297 (2000).
- [6] M. L. Mangano *et al.*, JHEP **0307** (2003) 001.
- [7] T. Sjöstrand, P. Eden, C. Friberg, L. Lonnblad, G. Miu, S. Mrenna and E. Norrbin, Comput. Phys. Commun. **135** (2001) 238.
- [8] T. Gleisberg, S. Hoche, F. Krauss, M. Schonherr, S. Schumann, F. Siegert and J. Winter, JHEP **0902** (2009) 007.
- [9] J. M. Butterworth, J. R. Forshaw and M. H. Seymour, Z. Phys. C **72** (1996) 637.
- [10] V. M. Abazov *et al.* [D0 Collaboration], Phys. Rev. Lett. **102** (2009) 192002.